Ultra Wide-Band : State of the Art; Implementation of a Performance-Controllable Low-Noise Amplifier

Serigne DIA, Balwant GODARA, Frederic ALICALAPA, Alain FABRE
Laboratoire IXL, Universite Bordeaux I, 33405 Talence-FRANCE
e-mail: dia@ixl.fr - godara@ixl.fr - alica@ixl.fr - fabre@ixl.fr

Abstract

Ultra Wide-Band (UWB) transmissions exhibit performances vastly superior to existing wireless systems - superlative data-rate capacity, high security, low cost, low power consumption - and are emerging as the hottest topic of research for upcoming wireless generations. This communication protocol is studied in detail, with mention of the history and estimates for the near future; the present and possible applications are mentioned; the advantages and unresolved issues are detailed; a typical UWB transceiver architecture is studied; the modulation and coding schemes are enumerated; and the possibility of long-range communication is touched upon. Finally, a new performance-controllable low-noise amplifier (LNA) destined for UWB systems is described. Inverse proportionality relations mean that better values are obtained for the noise figure, power consumption, bandwidth, and output impedance when the gain is higher. The amplifier was simulated in the 0.35 μm SiGe BiCMOS technology from ST Microelectronics. The gain of the LNA is controllable in the range from 0dB to 29dB; bandwidths of up-to 10GHz are obtained, covering the entire authorised UWB band; noise figures as low as 2.7dB are exhibited; the power consumption is always below 7mW; and an excellent temperature stability is shown - a gain drop of only 0.5dB in the temperature range from -40 °C to 85 °C.

Key Words: *Low-Noise Amplifier, Ultra Wide-Band.*

1. Introduction

Although it has an extensive history in military applications, the real impetus in the large-scale development and deployment of Ultra Wideband (UWB) was given by the February 14, 2002 Federal Communications Commission (FCC) ruling approving certain commercial deployment [1]. In Europe and Japan, although not yet finalized, its approval is in the process. The Institute of Electrical and Electronics Engineers (IEEE) has consecrated a team of experts to work towards the standardization of this new wireless communication protocol [2]. This team is expected to put forth its recommendations at the end of 2003. The UWB Working Group (UWBG) is an evolving association of companies, individuals, governing officials and regulators with a common goal of the development and acceptance of Ultra Wideband technology [3].

The deployment of UWB is of immense interest in telecommunications because of the superlative performances it is expected to give : a great improvement in data-rates and security accompanied by a corresponding reduction in cost, system complexity, and power consumption.

It is the aim of this paper to first summarize the major characteristics of this transmission standard. Beginning in section II we present a brief historical perspective of the standard, from its conception in the 1960s to its authorization by the FCC in 2002. This section will also attempt to chart a road-map for the future, judging from present trends and expert estimates. Section III then describes in more detail the definitions of the standard, the characteristics of the signals, and architectures of UWB transeivers. This will enable us to enumerate the various advantages and issues involved, along with the potential applications. In section IV, we move to the potential use of UWB for wireless communications, mentioning the technical details of the signals and the system architectures, and comparing them to those of a standard wireless communication system. We also discuss the various technologies used to implement different blocks of the system. Finally, section V proposes a low-noise amplifier (LNA) intended for use in emerging UWB systems. The results obtained from simulations of this LNA will be compared with those of other UWB LNA's in order to validate the present proposal. The paper ends with a brief discussion of the results in the light of requirements for UWB systems, and how far they satisfy these requirements.

2.   Historical Perspective and Future Roadmap

2.1.   History

The origin of UWB technology stems from work in time-domain electromagnetics begun in 1962 to fully describe the transient behaviour of a certain class of microwave networks through their characteristic impulse response. Instead of characterizing a linear time-invariant (LTI) system by the more conventional means of swept frequency, an LTI system could alternatively be fully characterized by its impulse response. However, it was not until the advent of the sampling oscilloscope and the development of techniques for sub-nanosecond (base-band) pulse generation, to provide suitable approximations to an impulse excitation, that the impulse response of microwave networks could be directly observed and measured [4].

In 1973, the first UWB communications patent was awarded. Through the late 1980's, this technology was alternately referred to as *base-band*, *carrier-free* or *impulse,* the term "ultra wideband" not being applied until approximately 1989 by the U.S. Department of Defence. In the United States, much of the early work in the UWB field (prior to 1994), particularly in the area of impulse communications, was performed under classified U.S. Government programs. Since 1994, however, some work has been carried out without classification restrictions, and the development of UWB technology has greatly accelerated.

In February 2002, the Federal Communications Commission (FCC) authorized the exploitation of UWB technology in the band 3.1GHz to 10.6GHz [1]. This was followed immediately by a great acceleration of work towards UWB chipsets, leading finally to the announcement of the first commercial UWB chipset, in June 2002, by Xtremespectrum (the "Trinity" chipset) [5]. Various other manufacturers have announced their own upcoming UWB modules [6].

2.2.   State of regulation and standardization

2.2.1.   Regulation

The principal pre-occupation of regulation authorities worldwide is the co-habitation of UWB with existing communications standards. Interference issues are pre-dominant, especially given the very large bands occupied by the signal, and its low power levels.

In the United States, the authorised exploitation of UWB is in the 3.1GHz to 10.6GHz band. Interference restrictions are very strict, but are likely to be eased because, in the words of the FCC, they are too restrictive and maybe even unnecessary. The transmitted power is at the moment limited to 75nW per megahertz [1].

The working group SE24 of the European Conference of Postal and Telecommunications Administrations (CEPT) has taken the charge to propose a frequency band for UWB systems in Europe. The European Telecommunications Standards Institute (ETSI) will establish the technical specifications for the utilisation of this band. These two authorities, in collaboration with various major industries, will release their final recommendations at the end of 2004 [7].

In Japan, regulation and normalisation authorities (MPT and MMAC) in consultation with industrial representatives have begun work on this question. Their findings and final recommendations will be released at the latest by 2004 [6].

2.2.2. Standardization

At the IEEE, the TG3a task group is working to develop the 802.11a standard [2]. The purpose of this group is to provide specifications for a low complexity, low cost, low-power consumption and high data rate wireless connectivity among devices within the Personal Operating Space. The data rate must be high enough (¿110Mbps) to satisfy set of consumer multimedia industry needs for WPAN (Wireless Personal Area Networks). UWB technology is the principal target of this future standard. At least 29 firms have already announced proposals.

The selected proposal must cover two modes of operation : 110Mbps and 200Mbps; higher bit rates, such as 480Mbps, are desirable. The desired range is 30ft for 110Mbps and can be reduced for higher bit rates. The system must be able to operate effectively in the presence of other 802.15.3a systems and in presence of other IEEE systems such as 802.11a. It is also important that the power consumption be low, to enable connectivity on battery operated portable devices.

2.3. UWB market

At present, the only UWB communications product available in the market is the "Trinity" chipset from Xtremespectrum [5]. Figure 1 shows a basic block diagram of this chipset. It uses a bi-phase modulation, the MAC protocol IEEE 802.15.3, and is able to attain speeds greater than 100Mbps. The technology of fabrication is the 0.18 μm SiGe BiCMOS. This chipset is characterised chiefly by its low power consumption. (around 200 mW).

Other firms are soon to follow suit, with the announcement of their own chipsets. There is likely to be a great upsurge in the UWB market, as illustrated in Figure 2, an estimate of the UWB chipset market up to 2007 [8]. The forecast is based on current trends and estimates by experts for the future. As can be seen from the figure, the UWB chipset shipments market is expected to reach 45 million units by 2007.

3. The UWB Standard

3.1. UWB definition

UWB transmission consists of the emission and reception of pulses of very short duration (typically 10 to 1000 pico-seconds). According to the FCC, a signal is considered UWB if its fractional bandwidth (FB) is

grather than 0.20, or bandwidth greater than 500 MHz [1]. The fractional bandwidth is defined by

$$FB = \frac{2(F_H - F_L)}{(F_H + F_L)} \tag{1}$$

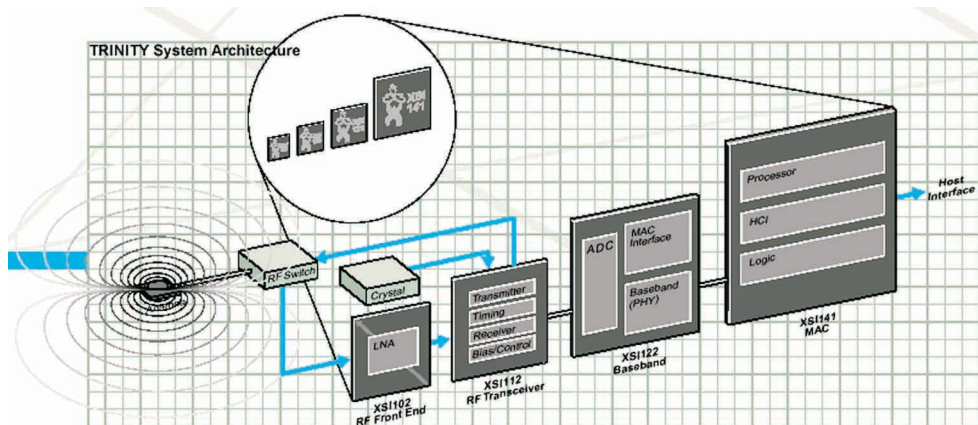where F_L and F_H and are, respectively, the lower and higher cut-off frequencies at –10dB.

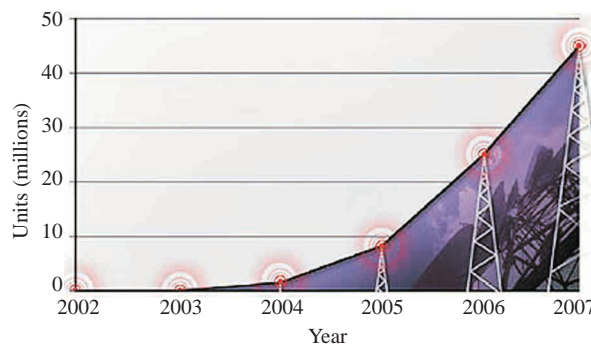**Figure 1.** Block diagram of the "Trinity" UWB chipset.

Figure 2. UWB chipset shipments market, moderate scenario

The short pulse-width corresponds to a large spectrum spread; the centre frequency of the spectrum is proportional to the inverse of the pulse duration. The major advantages of UWB transmissions stem from this fundamental property.

A classic example of a UWB signal is the Gaussian monocycle shown in Figure 3. This figure shows the signal in both time and frequency domains.

4
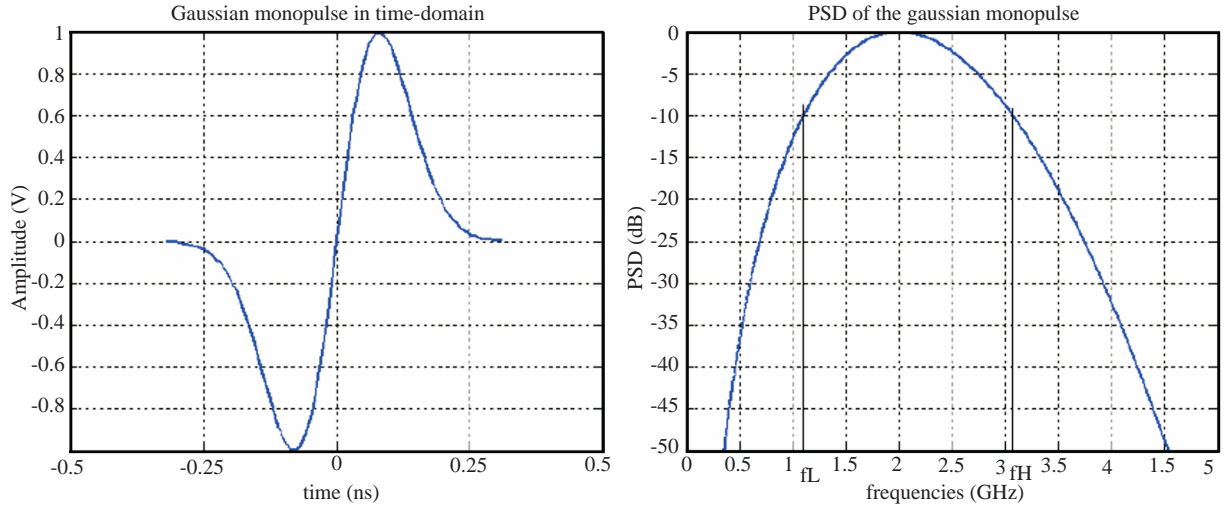
Figure 3. Gaussian monocycle in time and frequency domain.

The monocycle with a narrow pulse produces a wide bandwidth signal. The monocycle width determines the centre frequency and the bandwidth. In this example, a 0.5ns pulse width gives a centre frequency of 2GHz.

3.2. Modulation schemes

The regulatory limits placed on the power spectral density (PSD) of the transmitted signal affect the choice of the modulation scheme in two ways. First, the modulation technique has to be power-efficient; that is, the modulation needs to provide the best error performance for a given energy per bit. Second, the choice of a modulation scheme affects the structure of the PSD and thus has the potential to impose additional constraints on the total transmit power allowed [9].

A general UWB pulse train signal can be represented as a sum of pulses shifted in time, as shown in equation 2

$$s(t) = \sum_{k=-\infty}^{+\infty} a_k p(t - t_k) \tag{2}$$

where, s(t) is the pulse train signal;

p(t) the basic pulse shape;

a_k and t_k are the amplitude and time offset, respectively, of each individual pulse.

By varying the values of a_k and t_k, the information can be encoded in many ways.

3.2.1. Amplitude modulation

Pulse amplitude modulation (PAM) is based on the principle of encoding information with the amplitude of the impulses [10]. If we assume that pulses are uniformly spaced in time, we can rewrite equation (2) as:

$$s_{AM}(t) = \sum_{k=-\infty}^{+\infty} a_k p(t - kT) \tag{3}$$

where T is the period of pulse-spacing interval.

If a_k is always different from zero, the modulation scheme is called pulse amplitude modulation. Figure 4 shows this type of modulation. The two bits, "0" and "1", are specified by a certain level of amplitude : all pulses above this level are interpreted as "1", and all below by "0".
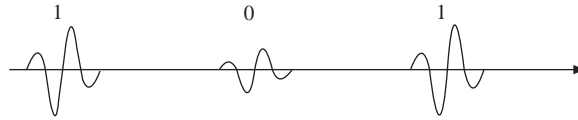
Figure 4. Pulse Amplitude Modulation (PAM)

On-off Keying modulation is a particular case of amplitude modulation, and it obtained when a_k can take the value 0, as shown in Figure 5
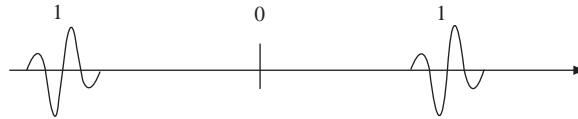
Figure 5. On-Off Keying modulation (OOK).

The power spectral density of this signal is the Fourrier transform of the signal autocorrelation. If we assume that the pulse weights correspond to the data bits to be transmitted and the data is random, we find that the PSD is as given by

$$DSP_{AM} = \frac{\sigma_a^2}{T}|P(f)|^2 + \frac{\mu_a^2}{T^2} \sum_{k=-\infty}^{+\infty} \left|P(\frac{k}{T})\right|^2 \delta(f - \frac{k}{T}) \tag{4}$$

where:

σ_a^2 and μ_a^2 are respectively the variance and the mean of sequences;

$P(f)$ is the fourrier transform of the basic pulse;

$\delta(f)$ is a unit impulse.

This PSD has both a continuous portion and discrete spectral lines. The presence of spectral lines can lead to reductions in total transmit power in order to meet regulatory PSD limits.

3.2.2. Pulse position modulation

Pulse position modulation (PPM) consists of encoding the data bits in the pulse stream by advancing or delaying individual pulses in time, relatively to some reference, as shown in Figure 6 [10].

Figure 6. Pulse position modulation (PPM).

In this case, the signal can be written as

$$s_{PPM}(t) = \sum_{k=-\infty}^{+\infty} p(t - kT + a_k \beta T) \tag{5}$$

where $a_k \in \{-1,+1\}$ is the data;

T is the reference interval between pulses;

β T is the amount of pulse advance or delay in time, relative to the reference position.

The interval between any two positions is made larger in order to avoid interference between symbols.

The PSD of this PPM signal is given by equation 6.

$$DSP_{PPM} = \frac{\sigma_a^2}{T}|B(f)|^2 + \frac{\mu_a^2}{T^2} \sum_{k=-\infty}^{+\infty} \left| M(\frac{k}{T}) \right|^2 \delta(f - \frac{k}{T}) \tag{6}$$

where B(f) is the fourrier transform of b(t)=0.5[p(t-T)-p(t+βT)];

M(f) the fourrier transform of m(t)=0.5[p(t-T)+p(t+βT)].

The modulation here tends to smooth the spectrum but this last still contains some spectral lines since the pulses are only delayed or advanced by a fractional part of the pulse width.

To reduce the level of the lines further, an additional dithering sequence can be added. Dithering is a pseudo-random process that jitters the reference position of the individual pulses according to a known random sequence. But dithering increases the level of complexity of a UWB system and adds to the synchronization schedule.

3.2.3. Bi-phase modulation

In bi-phase modulation (BPSK), information is encoded with the polarity of the impulses, as shown in Figure 7 [10]. The polarity of the impulses is switched to encode a "0" or a "1". In this case, only one bit per impulse can be encoded, because there are only two polarities available.
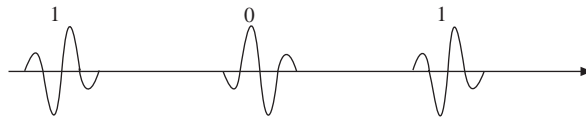
Figure 7. Modulation bi-phase (BPSK).

For this modulation scheme, values of the variance (σ_a^2) and the mean (μ_a^2) are respectively "1" and "0". Then the discrete portion of the PSD disappears as shown in equation 7.

$$DSP_{BPSK} = \frac{1}{T}|P(f)|^2 \tag{7}$$

This ability to eliminate spectral lines is a key feature of BPSK. It is crucial for UWB to minimise the presence of those spectral lines since they might interfere with conventional radio systems.

4.   Advantages and Potential Applications of UWB Transmissions

4.1.   Transmission capacity

As illustrated by its name, the large bandwidth occupied by the signal offers to UWB systems a very interesting property. The greater the occupied bandwidth, the greater is the transmission capacity (C), as shown by equation 8 [11].

$$C = B \log(1 + \frac{S}{N}) \tag{8}$$

where B is the bandwith;

S/N is the signal-to-noise ratio (SNR).

The capacity grows linearly with the band-width, but only logarithmically with the SNR. It is for this reason that the major applications of UWB technology are in the field of high data transmission like wireless networks. As shown in Figure 8, other standards now under development in the Bluetooth Special Interest Group and IEEE 802 working groups would boost the peak speeds and spatial capacities of their respective systems still further, but none appear capable of reaching that of UWB [11].
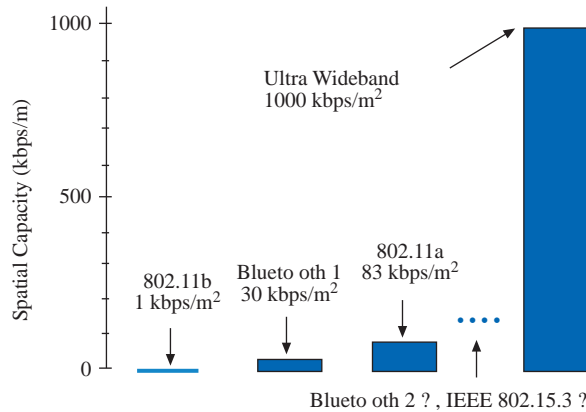
Figure 8. Spatial capacity of UWB and other systems.

4.2.   Other advantages

Another advantage of the wide band-width is the low power spectral density. Because the transmit power is spread over such a wide frequency band, the PSD of the signal is extremely low. This property was the mainstay for military applications, because it makes a transmission extremely difficult to detect. It also means minimal interference to other users in the same band and minimises possible risk to health [12].

A wide band-width is also reached in radar systems and positioning systems. For these systems, the greater the bandwidth, the better is the precision. Imaging systems are an offshoot of the original application (radar) and includes ground-penetrating radar, through-wall imaging and medical systems.

4.3.   Long-range applications

For UWB transmission, signal propagation depends on the "turnover point" d_c defined as [13].

$$d_c = \frac{4}{\lambda} h_T h_R \tag{9}$$

where λ is the wavelength of the centre frequency;

h_T and h_R are respectively the height of the transmit and receive antennas above the ground.

When the communication range is less than d_C, the signal is immunised from multi-path interference. Even indoors, minimum multi-path delays are some tens of nanoseconds, still much greater than the UWB pulse width. So the reflected signals never interferes with the main path and are entirely separable at the receiver. In fact, it is possible to use a RAKE receiver to combine the multi-path signals thus improving the SNR [12]. This property makes UWB ideal for wireless LANs and home-networking (i.e. indoor applications) and indeed, the first commercial applications of UWB are in this area.

When the communication range is greater than d_C, since the reflection coefficient is nearly –1 for low grazing angles, these small sub-nanosecond time differences between direct and reflected waves can result in substantial signal cancellation, even for short nanosecond pulses. The received power is approximately given by [13].

$$P_R = \frac{(h_T h_R)^2}{d^4} G_T G_R P_T \tag{10}$$

where

d is the distance between the emitter and the receiver;

G_T and G_R are respectively gains of transmit and receive antennas; and

P_T is the power emitted.

This equation exhibits a 4th law dependence on range, essentially independent of the operating frequency. In fact, to make a long range communication, the transmit power is very important. During recent development efforts for the US Navy, Multispectral Solutions developed a spectrally-confined high-power UWB transceiver which operates over the 30MHz to 50MHz portion of this band. These VHF UWB transceivers were designed with sufficient peak power output to achieve a communications range of 60 nautical miles over water [13].

4.4.   System Architecture

Compared to traditional radio transceiver architectures, the relative simplicity of UWB transceivers could yield important benefits. To explore these advantages, we consider the following traditional radio architecture, which will be contrasted with an example of a UWB architecture.

A contemporary example of a low-cost, short-range wireless architecture is the Bluetooth radio, an example of which is shown in Figure 9 [14].
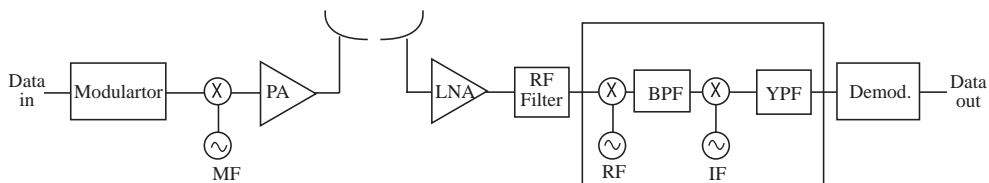

Figure 9. Bluetooth Super-heterodyne emitter-receiver.

Bluetooth uses a form of Frequency Shift Keying (FSK) where information is sent by shifting the carrier frequency high or low. This operation necessitates the use of Voltage-Controlled Oscillator (VCO) and Phase-Lock Loop (PLL). Before emission, the signal is sufficiently amplified by a power amplifier.

In receive mode, the extremely weak signal from the antenna is first amplified and then down-converted to an Intermediate Frequency (IF). The mixer produces a plethora of images of the desired signal where each image is centred at the sum and difference terms of the desired signal and the local oscillator (and harmonics of both). The image that falls at the desired IF frequency then passes through the IF filter, while the other images are rejected. At this low frequency, it is relatively easy to provide the stable high-gain circuits ($\sim$90dB) needed to demodulate the signal and recover the original information. In higher performance radio systems, such as cellular phones, two or even three down conversion stages may be employed. Most Bluetooth designs are based on variants of this super-heterodyne architecture with an emphasis on integrating as many functions as possible onto a single chip. In some designs, this includes the IF filters which make even Bluetooth's relatively relaxed channel selectivity requirements very difficult to realize over operating temperature [11].

We now look at a prototypical UWB transceiver as shown in Figure 10 [14]. This transceiver could be used for the same applications targeted for use with Bluetooth, but at higher data rates and lower emitted Radio Frequency (RF) power.
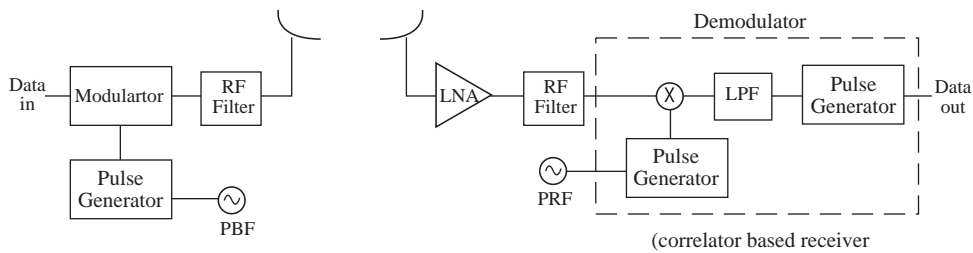
Figure 10. UWB emitter-receiver.

The information could be modulated using several different techniques (described above in part III.2). This modulated signal passes through a filter which gives it a suitable shape for the transmission. A power amplifier may not be required in this case because the pulse generator need only produce a voltage swing on the order of 100mV.

In receive mode, the energy collected by the antenna is amplified and passed through either a matched filter or a correlation-type receiver. A matched filter has an impulse response matched to the received pulse shape and will produce an impulse at its output when presented with RF energy which has the correct (matching) pulse shape. The original information is then recovered with an adjustable high-gain threshold circuit.

We notice the relative simplicity of this implementation compared to the super-heterodyne architecture. This transceiver has no reference oscillator, Phase-Lock Loop (PLL) synthesizer, VCO, mixer, or power amplifier. This simplicity translates to lower material costs and lower assembly costs.

However, there are still some design challenges for UWB systems. Issues such as low noise amplifier, filter matching accuracy and the extreme antenna bandwidth requirements can often be difficult to achieve.

4.5.   LNA in the UWB receiver block

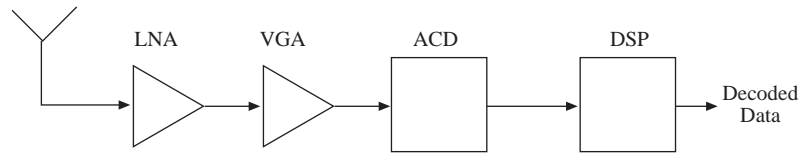Figure 11 presents a prototype of a UWB receiver [15].

Figure 11. Standard UWB Receiver Architecture.

The stringent requirements for UWB systems place particular emphasis on each element of the receiver. The low-noise amplifier (LNA) as a stand-alone product is required to provide a flat gain response from DC up-to several gigahertz (GHz), very low signal distortion, low current consumption, and high signal voltage gain transfer. Constituting the first block in the receiver chain, the noise figure of the LNA adds directly to that of the entire system, and thus has to be very small. In addition to the LNA, the UWB receiver architecture contains a variable-gain amplifier (VGA) which is necessary for the control of the signal being passed on to the base-band section.

LNAs are traditionally implemented using voltage-mode techniques. Bipolar technologies have proven very efficient for LNAs. In the section that follows, we will apply a new approach – the current-mode approach – to the design of the LNA. The module will incorporate the functions of LNA and VGA into a single unit, thus eliminating the need for a separate component. It will be shown in the course of the following section that the mode offers several advantages, excellently suited to the upcoming UWB standard.

5.   A LNA for UWB Receiver Systems

5.1.   System constraints vis-à-vis LNA

5.1.1.   Gain

In radio-frequency (RF) blocks, the gain G_T is most commonly defined in function of the Scattering parameters (S-parameters) and the reflection coefficients at the source (Γ_S) and load (Γ_L) [16].

$$G_T = \frac{|S_{21}|^2(1 - |\Gamma_S|^2)(1 - |\Gamma_L|^2)}{|(1 - S_{11}\Gamma_S)(1 - S_{22}\Gamma_L) - S_{12}S_{21}\Gamma_L\Gamma_S|^2} \tag{11}$$

For narrow-band amplifiers, the peak gain is normally considered the indicator, and is evaluated when the coefficients of reflection at the input and output are zero. However, for UWB systems, where a stable gain is desired over a large band, it is difficult to maintain a steady gain if we cancel out the reflection coefficients. The peak gain thus has to be reduced, in order to obtain an optimal and acceptable performance over a large frequency band.

5.1.2.   Noise figure

As mentioned earlier, the LNA noise figure adds directly to that of the receiver, and dictates the minimum detectable signal (MDS) for the antenna [16].

$$MDS = -174dBm/Hz + NF + 10.\log BW + SNR\min \tag{12}$$

where
NF is the noise figure of the receiver;

BW is the bandwidth;

SNR_{min} is the signal-to-noise ratio at the reception end.

The noise factor F of a quadripole whose input generator has an impedance of Z_g ($Z_g = R_g + jX_g$) is expressed as the degradation of the signal as it traverses the quadripole [17].

$$F = \frac{(S/N)_s}{(S/N)_e} \tag{13}$$

This can be expressed as:

$$F = F_{\min} + \frac{|Z_g - Z_{g_0}|^2}{R_n R_g} \tag{14}$$

where F_{min} is the minimum noise factor;

Z_{g0} ($Z_{g0} = R_{g0} + jX_{g0}$) is the optimal impedance: the value of Z_g for which the noise factor is minimum (F_{min});

R_O is the equivalent noise resistance of the quadripole.

Practically, the internal noise of the quadrapole is a function of various types of internal noise sources, and R_O represents the equivalent impedance of the ensemble of these sources, taken to be purely resistive. The noise figure NF is the decibel expression of the noise factor:

$$NF = 10. \log F \tag{15}$$

5.1.3. Dynamic range

The linearity of a narrow-band component can be expressed in two ways : by its dynamic range, or its third-order intercept point (IP_3) [16]. The IP_3 determines the interference between two equal signals of neighboring fundamental frequencies. For UWB systems, however, where the signal occupies a very large band, there are no fundamental frequencies, and thus there is no IP3 for such systems. The dynamic range is thus taken as the indicator of component linearity. This range is determined starting from the 1dB compression point (P_{1dB}). If G is the power gain of the LNA, and P_{in} and P_{out} respectively the powers of the input and output signals,

$$P_{out}(dBm) = P_{in}(dBm) + G(dB) \tag{16}$$

The graphic representation of $P_{out} = f(P_{in})$ is a straight line with a slope of +1 and an offset of G_{dB}. The point $P_{out,MDS}$ will then represent the output signal when the input is $P_{in,MDS}$. As P_{in} increases, the amplifier tends to saturate, and the output power tends towards a constant value where it becomes independent of the input signal. The 1dB compression point ($P_{in,1dB}$, $P_{out,1dB}$) is the point where the difference between the actual P_{out} and the expected P_{out} is 1dB. The dynamic range of the amplifier is thus defined by

$$d_R = P_{out,1dB} - P_{out,MDS} \tag{17}$$

5.2.   Schematic

Figure 12 presents the schematic of the current-mode LNA [18].
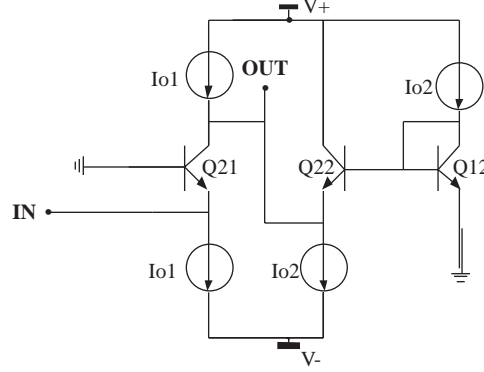
Figure 12. Base schematic of the LNA.

This design of this current-mode LNA is based on the operation of the controlled current conveyor in trans-conductor mode.

The final configuration of Figure 12 uses the minimum number of NPN transistors possible, three, to convey the signal, allowing for higher bandwidths to be obtained, and improving the noise performance. Other than the transistors, the LNA uses no active components. The NPN transistors are polarized by the two dc current sources I_{O1} and I_{O2}.

5.2.1.   Gain

The input voltage signal is applied at the point labeled "IN", on the emitter of Q_{21}. And the output signal is tapped at "OUT", the point of common connectivity of the collector of Q_{21} and the emitter of Q_{22}. The equivalent schematic of the LNA permits a theoretical study of its characteristics. This is given in Figure 13.
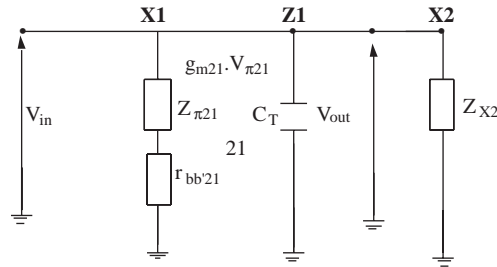
Figure 13. Small-signal equivalent of the LNA.

The base resistances of the transistors Q_{21} and Q_{22} being sufficiently low to not show any inductive elements, the gain G(s) of the amplifier can be expressed as

$$G(s) = \frac{V_{out}}{V_{in}}(s) = \frac{g_{m21}}{g_{m22} + C_T s} \qquad (18)$$

Here, C_T represents the influence of the parasitic capacitances of the transistors; gm_{21} and gm_{22} are, respectively, the trans-conductances of transistors Q_{21} and Q_{22}.

13

This expression exhibits a single pole, situated at the frequency $f_p = g_{m22}/2\pi C_T$. The rebound is found at higher frequencies when C_T is lower. A compromise thus has to be made on the sizes of the transistors (which define C_T) in order that the bandwidth is sufficiently large, and the rebound negligible. The gain can also be expressed as

$$G = \frac{g_{m21}}{g_{m12}} = \frac{I_{01}}{I_{02}} \tag{19}$$

This equation shows that the gain is controllable by variation of currents I_{01} and I_{02}. C_T depending on the polarisation currents, the expression for the frequency pole shows that the pass-band of the LNA is an inverse function of I_{02}.

5.2.2. Noise

The major part of the noise in the amplifier is contributed by the input transistor Q_{21}. When the source resistance R_s is adapted to the input impedance of the amplifier, the noise factor is given by

$$F = 1 + \frac{r_{bb21}}{R_S} + \frac{1}{2} \tag{20}$$

where r_{bb21} represents the base resistance of transistor Q_{21}.

The noise figure thus tends towards a minimum value of 1.77dB, when the value of r_{bb21} is zero.

5.2.3. Impedances

In the base frequency region, the simplified expression of the input impedance Z_{in} of the amplifier is given by

$$Z_{in} = \frac{1}{g_{m21}} + \frac{r_{bb21}}{\beta_{21}} \tag{21}$$

This shows that the input impedance of the amplifier depends on I_{01}. In all simulations, this current was thus maintained at a constant value, in order that the input impedance remains constant at $50\,\Omega$.

Ignoring parasitic effects, the theoretical expression for the output impedance Z_{out} of the LNA is

$$Z_{out} = \frac{1}{g_{m22}} \tag{22}$$

Z_{out} thus depends on I_{02}. In systems where the LNA is totally integrated into the reception system, an impedance adaptation to $50\,\Omega$ at the output is no longer necessary.

5.3. Simulations

5.3.1. Technology

SiGe technology is characterized by a high dynamic range and low noise. Moreoever, the transition frequency f_T of the NPN transistors is much higher than that for the classical silicon NPN. The compatibility of the

technology with CMOS processes offers several important advantages from the economic stand-point because of the low cost of CMOS. A BiCMOS technology is thus well adapted for design and implementation of high-frequency mixed-signal components.

The LNA presented above was simulated in the 0.35 μm SiGe BiCMOS from ST Microelectronics. In this technology, the bipolar NPN transistors have a transition frequency of around 40GHz. The current gain of these transistors approaches 90, and the Early voltage is around 60 volts. Also available in this technology are vertical and lateral PNP transistors, the former of which have a much lower f$_T$ of 4GHz.

5.3.2. Simulated circuit

The LNA performance depends on the quality of the current mirrors used to substitute the current sources. Various possibilities were studied and simulated. Utilization of vertical PNP current mirrors severely limits the bandwidth of the LNA because of the very low f$_T$ of these transistors. Additionally, these transistors generate more noise than NPN. Current mirrors made of lateral PNP transistors, while immensely improving bandwidth characteristics, still contribute too much noise, which raises the noise figure of the LNA to unacceptable levels. Towards improving this performance, mixed mirrors, comprising bipolar and CMOS transistors were also studied. The best solution for the biasing circuit finally obtained was the use of MOS mirrors. The final schematic of the LNA, after substituting MOS mirrors for the current sources, is given in Figure 14.

Figure 14. Simulated schematic of the LNA.

The dimensions of the transistors were varied, until a final set of values was arrived at which gives the optimum performance for the various parameters. The bias voltage used for the circuit was ± 1.5 V. As mentioned earlier, the input impedance of the LNA is a function of I$_{O1}$. This current was thus kept constant, at 525 μA, a value which gives an input impedance of 50Ω. I$_{O2}$ was varied, thus giving a method to control the performance of the LNA.

5.3.3. Input signal

In order to determine the performance of the LNA for UWB, the input signal used was a train of 1ns width and ± 10 μV amplitude (corresponding to signal power around –90dBm) bi-phase pulses, with the impulses
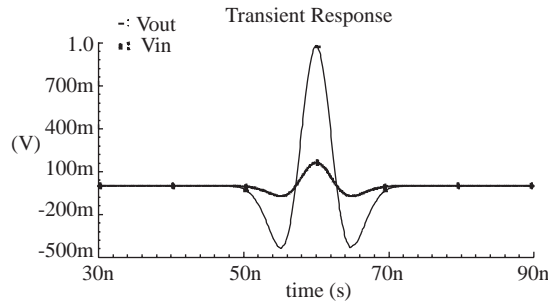
being right side up for 1, and upside down for 0. These impulsions are second derivatives of the Gaussian function.

## 5.4. Simulation results

5.4.1. Transient response

Figure 15 represents the signal at the input and the output of the LNA, for an AC gain value of 20dB.

Figure 15. Transient response of the LNA to a double-derived Gaussian pulse; with $V_{DC} = \pm 1.5$ V, $I_{O1} = 525$ μA, and gain = 20dB.

5.4.2. AC gain

Figure 16 represents the AC gain of the amplifier, for different values of the polarization current I_{O2}, I_{O1} being fixed at 525 μA.
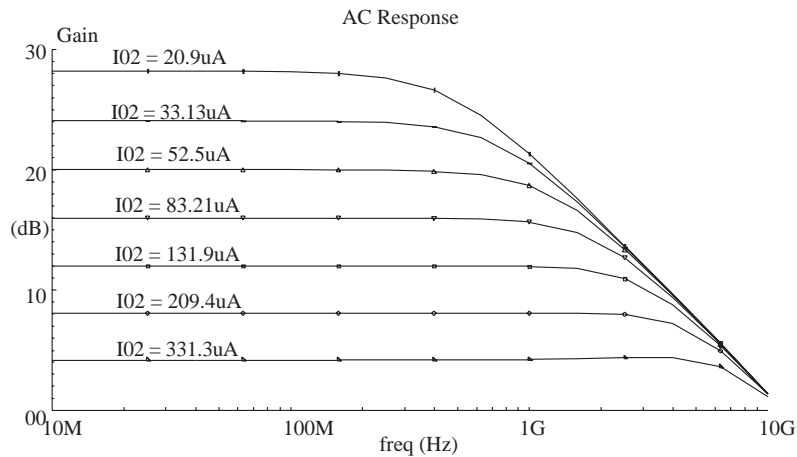
Figure 16. AC Response of the LNA for different values of I_{O2}; with $V_{DC} = \pm 1.5$ V, and $I_{O1} = 525$ μA.

This figure shows that the LNA has a stable gain profile for very large bands. Additionally, there are no rebounds for gains greater than 9dB, and these rebounds rest negligible for other values of the gain. (for example 0.3dB at 2.2GHz, for a gain of 8dB). For a standard gain of 15dB, the pass-band obtained ranges from DC to 2.3GHz.

5.4.3. Noise figure

Figure 17 below shows the noise figure profiles of the LNA for various values of I_{O2}. As before, I_{O1} is fixed at 525 μA. As can be seen, the noise figure shows a direct variation with I_{02}. That is, the noise figure reduces as the gain increases.
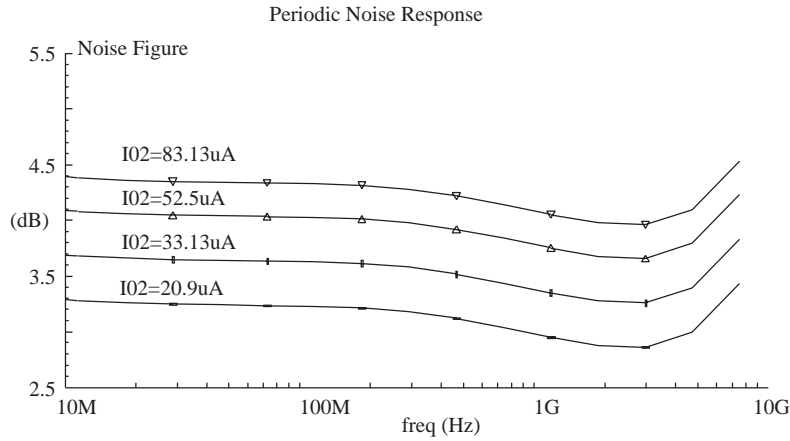
Figure 17. Noise figure of the LNA for different values of I_{O2}; with $V_{DC} = \pm 1.5$ V, and $I_{O1} = 525$ μA.

5.4.4. Input impedance

The adaptation of the input impedance to 50Ω is obtained by fixing I_{01} .to 525 μA. Figure 18 below shows the variation of Z_{in} as function of frequency.
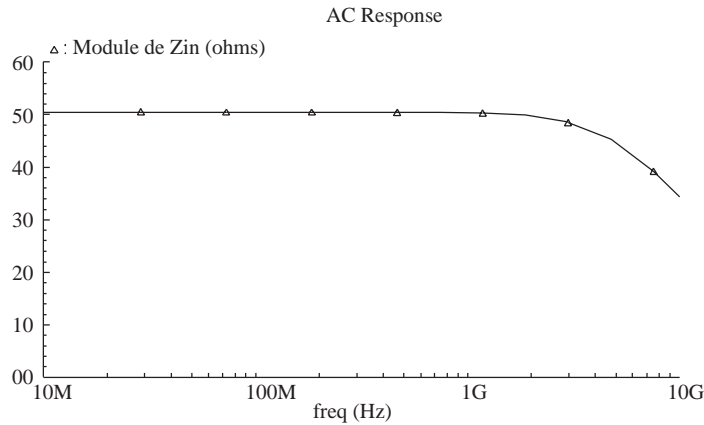
Figure 18. Magnitude of Z_{in}; with $V_{DC} = \pm 1.5$ V, and $I_{O1} = 525$ μA.

The input impedance rests around 50Ω, almost purely resistive, up-to frequencies of 2GHz.

5.4.5. S_{11}

The input adaptation of the LNA can also be illustrated by the scattering parameter S_{11} which presents the reflection coefficient at the input. Figure 19 below shows the variation of S_{11}, I_{01} being equal to 525 μA.
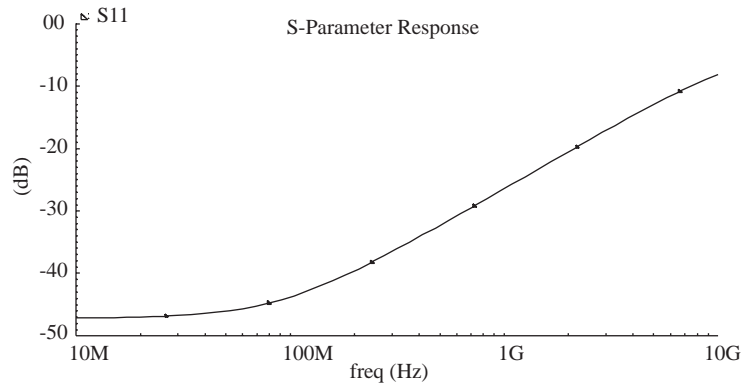
Figure 19. Magnitude of S_{11}; with $V_{DC} = \pm 1.5$ V, and $I_{O1} = 525$ μA.

In the base frequency region, S_{11} remains very low (-48dB@10MHz), and it stays lower than –10dB for frequencies up-to around 4GHz.

5.4.6. Output impedance

As mentioned, Z_{out} is a function of I_{O2}. This is illustrated by Figure 20, which shows the frequency variation of the modulus of Z_{out} for different values of I_{O2}.
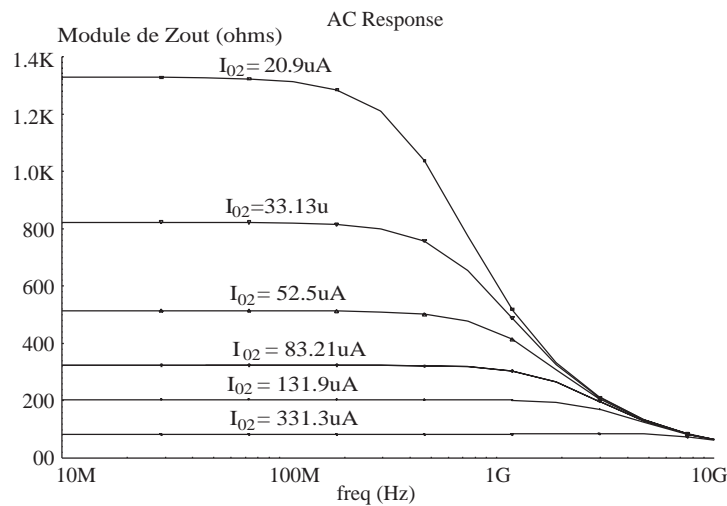

Figure 20. Magnitude of $Z_{out,}$ for different I_{O2}; with $V_{DC} = \pm 1.5$ V, and $I_{O1} = 525$ μA.

5.4.7. 1dB compression point

Figure 21 gives the 1dB compression point, referred to the input, for $I_{02} = 83$ μA, at a signal frequency of 2GHz. This parameter is important in determining the dynamic range of the LNA.

For $I_{01} = 525$ μA and $I_{02} = 83$ μA, P_{1dB} is around 12dBm. This is an important value towards validating the LNA for use in UWB systems, where the signal levels are very low.
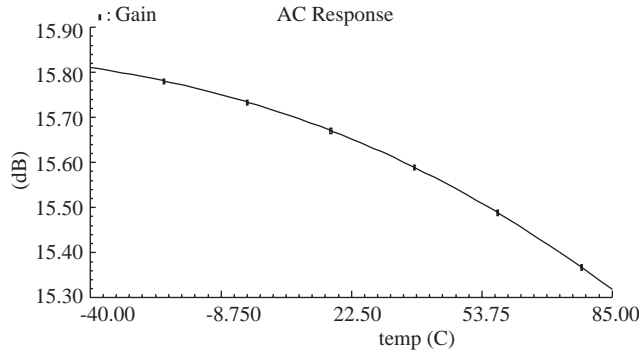
5.4.8. Temperature stability of the LNA

From a practical point of view, it is important that the components give a reliable and stable performance for a wide range of operating temperature. Actual operating conditions tend to vary appreciably from the

Periodic Steady State Response
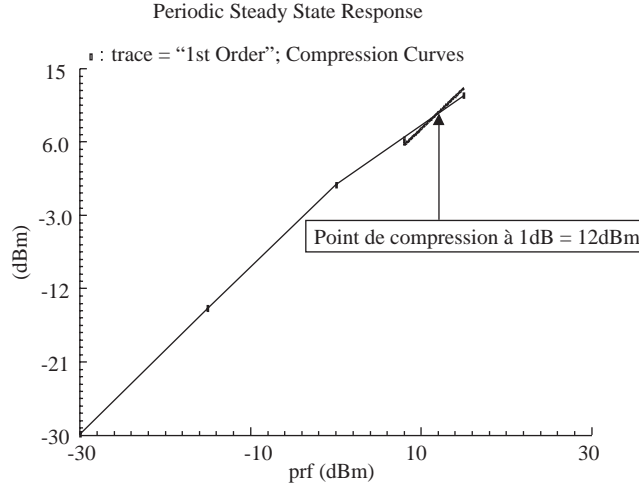
Figure 21. Input P_{1dB} with $I_{O1} = 525$ μA, $I_{O2} = 83$ μA, and $V_{DC} = \pm 1.5$ V.

standard 25 °C point, especially because of heating effects. Figure 22 shows the gain of the LNA as a function of temperature.

AC Response

Figure 22. Variation of AC gain with temperature; with $I_{O1} = 525$ μ A, $I_{O2} = 83$ μ A, and $V_{DC} = \pm 1.5$ V.

The LNA has an excellent temperature stability, as is proved by the fact that its gain drops only by 0.5dB in the entire temperature range of –40 °C to +85 °C.

5.5.   Performance Summary

Table 1. summarises the principal characteristics of the LNA in function of I_{02}, with I_{01} fixed at 525 μ A, and the bias voltage being $\pm$ 1.5 V.

The gain and bandwidth vary inversely with one another. As the gain reduces from 29dB to 12dB, the pass-band of the LNA passes from 0.5GHz to 3.7GHz. The noise figure remains in all cases lower than 5.0dB. The noise figure and the current consumption reduce as the gain increases: as the gain passes from 12dB to 29dB, the noise figure changes from 5dB to 2.7dB, and the power consumed from 7.1mW to 4.8mW. Additionally, the rise in gain is accompanied by a reduction in the dynamic range of the LNA: the 1dB compression point is 13.7dBm when the gain is 12dB whereas it rises to 7dBm at a gain of 29dB.

Table 2 sums up the performance of the LNA at a moderate gain of 16dB (at $I_{O2} = 83$ μA). The gain is a flat frequency response of 16dB, with no rebound, up-to high bands, as shown by the bandwidth.

19

Table 1. Summary of LNA performance; with $I_{O1} = 525$ μA, and $V_{DC} = \pm$ 1.5 V.

I_{O2} (μA)	Gain (dB)	Bandwidth (GHz)	NF (dB)	Consumption (mW)	Input P_{1dB} (dBm)
21	29	0.5	2.7	4.8	7.0
33	24	0.9	3.4	5.4	8.3
53	20	1.4	4.1	5.8	11.4
83	16	2.3	4.4	6.2	12.0
132	12	3.7	5.0	7.1	13.7

Table 2. Performance synopsis at AC gain of 16dB.

Technology	SiGe BiCMOS 0.35μm
Transition frequency	40 GHz
Gain control	0dB to 29dB
Mode of gain control	Current
Gain	16 dB
Rebound	0
Bandwidth (-3dB)	DC – 2.3 GHz
Centre Frequency	3.35 GHz
NF	4.4 of dB
$\mid S_{11} \mid$	-21 dB
$\mid S_{12} \mid$	-63.5 dB
Input P_{1dB}	12dBm
THD (at Vin=10μV)	0.5%
Offset (at Vin=10μV)	0.01μV
$\mid Z_{IN} \mid$	50 Ω
$\mid Z_{OUT} \mid$	280 Ω
Current Consumption	4.2 mA
Bias Voltage	$\pm$1.5 V

Further indications of the excellent signal quality are given by the harmonics and inter-modulation products : the second-order harmonic is 88dB lower than the primary, the third order inter-modulation product is 85dB lower than the principle peak.

The LNA has a stable temperature performance, showing a drop in simulated gain of only 0.5dB in the range –40 °C to +85 °C, and a simulated bandwidth dip of only 0.1GHz in the temperature range of 0 to 85 °C.

5.6.   Comparison with other UWB LNAs

Table 3 compares the performance of the LNA presented here with two other recent UWB LNAs. All three have been realised in the SiGe BiCMOS technology, allowing a direct comparison. The first of these was published as part of a thesis dissertation, and the second is a component of the Trinity chipset from XtremeSpectrum, the first UWB chipset in the market.

As can be seen, the gain control range is the largest for the current LNA proposal. The maximum band-width that can be obtained is inferior to that for [15], but vastly superior to the Trinity chipset, and effectively covers the entire authorised UWB band. The noise figure is comparable to the other two. The power consumption is by far the lowest, allowing efficient performance for low dissipation, an important criteria.

Table 3. Comparison of LNA performance with two other recent UWB LNA.

Parameter	LNA-[15]	LNA-[5]	This work
Technology (μm)	0.18	0.5	0.35
Gain (dB)	0 to 20	0.1 to 8.4	0 to 29
BW (GHz)	3.1 to 10.6	0.8 to 1.6	0 to 10
NF (dB)	5.6, max	3.0	2.7 to 5.5
Supply (V)	3.3	3.3	1.5
Consumption (mW)	200 (module)	23.1	7, max

5.7. Discussion

A current-mode LNA has been simulated in a low-cost $0.35\,\mu$m SiGe BiCMOS technology. The gain provided is controllable in the range 0dB to 29dB; and the inverse relation of the bandwidth to the gain provides a way to trade off these two important parameters according to need, and to adapt the LNA to UWB systems. The gain control also eliminates the need to have a VGA in the receiver chain. At a moderate gain of around 16dB, the LNA exhibits -3dB bandwidth of DC to 2.3GHz; further, a trade-off between gain and bandwidth allows pass-bands greater than 10GHz, thus effectively covering the bounds of the authorized UWB band, while contributing a low noise figure and consuming little power. The distortion introduced to the signal is negligible. The low cost of the technology used, the low number of active components, the absence of external components, the constant $50\,\Omega$ input impedance, stable temperature performance, and the versatility introduced by performance control, prove the excellent potentiality of the present LNA for emerging UWB systems.

6. Conclusion

In this paper, we have made a brief review of the various properties, issues and facets of emerging Ultra Wide-Band systems. Currently used for short-range purposes, these transmissions are likely to find their domain of application extended to long-range communications, and perhaps even replace existing mobile communications systems. The state of the art at the present moment has been updated; the philosophy of information transmission in the form of pulses has been described; the modulation schemes are also mentioned. Thereafter, the system-level architecture for UWB has been introduced and then compared to that of existing wireless communications protocols. Towards the design of UWB transceiver modules, a new topology for the Low-Noise Amplifier has been introduced. This performance-controllable amplifier incorporates the functions of a low-noise amplifier and a variable-gain amplifier, towards simplifying the receiver architecture. This SiGe BiCMOS LNA has pass-bands extending the entire authorised UWB band; a gain control range of around 30dB; low noise figures; high temperature stability; extremely low power consumption; and a constant $50\,\Omega$ input impedance. The excellent performance is reasserted on comparison with two other LNA modules designed for UWB systems.

References

[1] "In the matter of Revision of part 15 of the Commission's Rules Regarding Ultra-Wideband Transmission Systems", FCC, available on:

http:/www.uwb.org/files/new/FCC_RandO.pdf

[2] "IEEE 802.15 WPAN High Rate Alternative PHY Study Group 3a (SG3a)", available on:

http://grouper.ieee.org/groups/802/15/pub/SG3a.html

[3]] Ultra Wide Band Working Group, available on:

http://www.uwb.org

[4] R.J Fontana, "A brief history of UWB communications", Multispectral Solutions, available on:

http://www.multispectral.com/history.html

[5] "Trinity for media-rich wireless applications", XtremeSpectrum, available on:

http://www.ieee.com/archive/uwb.pdf

[6] "Cover Story : UWB emerges as standard for wireless home", Nikkeil Electronics Asia, April 2003, available on

http://neasia.nikkeibp.com/nea/200304/comnet_238948.html

[7] "Report of the WGSE meeting, 12-16 May 2003, Cavat (Croatia)" available on:

http://www.ero.dk/EEE33BA9-4252-AD6C-7BE7EFB81898.W5Doc

[8] "Ultra Wideband can find relief from CE industry", Allied Business, available on:

http://www.alliedworld.com/selvets/Research Details?productid=UWB

[9] Matt L. Welborn, "Efficiently modulate UWB signals", Microwave and RF magazine, September 2002, pp 59-65

[10] "New Ultra-wideband technology", Discrete Time Communications, available on:

http://www.discretetime.com/index_files/page0003.html

[11] J. Foerster, E. Green, S. Somayazula and D. Leeper, "Ultra-Wideband Technology for Short or Medium Range Wireless Communications", available on:

http://developer.intel.com/itj/q22001/pdf/art_4.pdf

[12] Ultra Wide Band, available on:

http://www.twocultures.org

[13] R. Fontana, A. Ameti, E. Richley, L. Beard et D. Guy, "Recent advances in ultra wideband communication systems", Multispectral Solutions.

[14] J. Foerster, "Ultra-Wideband Technology, high-rate wireless communications", available on:

htttp://www.ieee.or.com/Archive/uwb.pdf

[15] W. Namgoong, "Ultra Wideband Digital Reciever-LNA design", University of Southern California, September 2002, available on:

http://www.ultra.usc.edu/new_site/MURI/namgoong0502pptpdf.pdf

[16] S. Lee, "Design and analysis of ultra-wide bandwidth impulse radio receiver", Thesis towards Doctor of philosophy (electrical engineering), University of southern California, August 2002.

[17] A. Pacaud, "Electronique radiofrequence', Editor Ellipses, March 2000, pp. 64-66.

[18] F. Seguin, "Etude et realisation de circuits convoyeurs de courant de seconde generation en technologie BiCMOS. Application a l'amplification RF reglable ", Thesis towards Doctor of Philosophy, Universite Bordeaux 1, December 2001, Bordeaux, France.